Observation of Electronic States on Si(111)-(7 × 7) through Short-Range Attractive Force with Noncontact Atomic Force Spectroscopy

T. Arai[1,2] and M. Tomitori[1]

[1]*Materials Science, Japan Advanced Institute of Science and Technology, Ishikawa 923-1292, Japan*
[2]*PRESTO, Japan Science and Technology Agency, Saitama 332-0012, Japan*

(Received 5 August 2004; published 13 December 2004)

We experimentally reveal that the short-range attractive force between a Si tip and a Si(111)-(7 × 7) surface is enhanced at specified bias voltages; we conduct force spectroscopy based on noncontact atomic force microscopy with changing bias voltage at a fixed separation. The spectra exhibit prominent peaks and a broad peak, which are attributed to quantum mechanical resonance as the energy levels of sample surface states are tuned to those of the tip states by shifting the Fermi level through changing bias voltage, and to the resonating states over a lowered tunneling barrier, respectively.

DOI: 10.1103/PhysRevLett.93.256101 PACS numbers: 68.37.Ps, 73.20.–r, 81.05.Cy

The adhesive force between two solid bodies at close separations is one of the most fundamental interactions in condensed matter, which involve chemical bond, metallic bond, van der Waals force, electrostatic force, and so on. For a simple case of chemical covalent bonding between two isolated atoms, Pauling successfully introduced the concept of quantum mechanical resonance between their electronic states at close energy levels [1]. By extending this concept of the resonance to condensed matter, the force interaction between two bodies at small separations can be regarded as the resonating overlap of their electron wave functions.

Since the advent of scanning tunneling microscopy (STM) [2] and atomic force microscopy (AFM) [3], the adhesive force and the tunneling conductance between two bodies have simultaneously been examined by bringing a tip closer to a sample, i.e., by taking force-distance curves [4]. For the correlation between the force and the tunneling current, Chen theoretically evaluated it on the basis of the quantum mechanical resonance between the surface electronic states of both tip and sample through the tunneling barrier [5]. The force and the tunneling conductance can be derived from the overlapping of their wave functions at close energy levels through a tunneling barrier: the Bardeen's matrix element, which is used to evaluate the tunneling current, is fundamentally equal to the Heisenberg's resonance energy E, corresponding to the covalent bonding. The correlation between the force and the tunneling current has been shown experimentally for metals [6–8], but it is still under debate: the decay length of force is larger than that of typical chemical interactions, and the patched charges around a tip may change the interaction.

It is noted that the energy level of the surface electronic state in one body of condensed matter can be shifted relatively with respect to the other by changing bias voltage, corresponding to the Fermi level shift. Since the resonance occurs between the electronic states having closer energy levels, the quantum mechanical resonance is expected to be enhanced by tuning the energy levels of surface electronic states in the two bodies through the Fermi level shift. Thus, the interaction between two bodies should be analyzed by force spectroscopy with a capability of changing bias voltage.

The noncontact (nc)-AFM [9] has demonstrated its excellent capabilities with a high force sensitivity to obtain atom-resolved images [10] and measure the force interaction [11]. We found that the atomic contrast in nc-AFM images of Si(111)-(7 × 7) is site-selectively enhanced at a specific bias voltage [12]. This implies that the strong bonding is induced when the energy levels of sample surface states are tuned to those of tip states by changing the bias voltage. Conversely the surface states concerning the chemical bonding can be analyzed by taking force-voltage curves at a fixed separation. In this Letter we present a novel spectroscopic method with changing bias voltage for the short-range force between two bodies at close separations on the basis of nc-AFM, termed noncontact atomic force spectroscopy (nc-AFS). The nc-AFS spectra exhibit prominent peaks at specific bias voltages at close separations, which are attributed to quantum mechanical resonance.

To conduct the nc-AFS, we used a homemade nc-AFM in 5×10^{-11} Torr operated at room temperature with a piezoresistive Si cantilever having a [001]-oriented Si tip, cleaned by several treatments including heating in ultrahigh vacuum (UHV) [13]. Since we used no laser optics to detect the cantilever deflection, dark environmental conditions were realized in the nc-AFM chamber; light irradiation may affect the electronic states at semiconductor surfaces of both the tip and a sample. To depict surface topography, the cantilever of nc-AFM is oscillated at a constant amplitude with a self-oscillation circuit at its resonance frequency f, and scans the tip over a sample surface at close separation under a constant shift of the resonance frequency Δf, which is measured by a frequency modulation technique. On nc-AFS measurement, the resonance frequency shift Δf indicating the

change in force is recorded at a constant oscillation amplitude by changing bias voltage between the tip and sample in a triangular sawlike waveform with a duration of 50 ms, while stopping the tip scan and holding the tip-sample separation instantaneously, which is similar to the STM-based current imaging tunneling spectroscopy [14]. A sample of n-Si(111):P-(7×7) was cleaned by flashing at 1200 °C in UHV.

Figure 1 shows a nc-AFM image of Si(111)-(7×7): bright spots correspond to Si adatoms and a few dark regions to defects. For nc-AFS measurements, we selected the tip position over the middle of a wide terrace ~50 nm, because the force interaction could be changed near the steps [15,16]. Under the imaging conditions as in Fig. 1, the Si adatoms in the faulted half unit cell are depicted slightly higher than in the unfaulted half unit cell. This tendency coincides with the site dependence of electron density on Si(111)-(7×7) predicted by an *ab initio* calculation [17]: the force roughly depends on the electron density at each atomic site. However, we found that the atomic corrugation in nc-AFM images changes with bias voltage [12,18]. This implies that the image contrast depends not only on the atomic position but also on the electronic states, and the detailed analysis with changing bias voltage is needed.

By applying a bias voltage between the tip and the sample, it is widely known that long-range attractive force F_V is induced electrostatically. In general the total force F_{total} between the tip and the sample can be expressed as $F_{\text{total}} = F_V + F_{\text{vdw}} + F_{\text{bond}} + F_{\text{repul}}$; here F_{vdw} is the van der Waals force, F_{bond} the chemical bond between an atom at the tip apex and an atom on the sample surface, including the metallic adhesion, and F_{repul} the repulsive force due to core-core interaction with exchange interaction. F_V and F_{vdw} are long-range forces, and F_{bond} and F_{repul} are short-range forces. The resonance frequency shift Δf, measured by the nc-AFM, can be expressed for force F as [19]

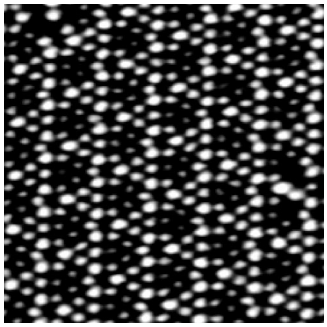

FIG. 1. Nc-AFM image of a Si(111)-(7×7) surface. Brighter six Si adatoms are in a triangle half unit cell of 7×7, referred to as a faulted half unit cell, and darker six adatoms in an unfaulted half unit cell. Imaging conditions: spring constant of the cantilever $k = 10$ N/m, $\Delta f = -40$ Hz ($f_0 = 192$ kHz), oscillation amplitude $A = 18$ nm, sample bias voltage $V_{\text{sample}} = -0.6$ V, and scanning area 14×16 nm.

$$\Delta f = \frac{f_0}{2\pi kA} \int_0^{2\pi} F(z_0 + A\cos\varphi)\cos\varphi \, d\varphi. \quad (1)$$

Here k and f_0 are the spring constant and the resonance frequency of the cantilever at free, respectively, A the oscillation amplitude of the cantilever, and z_0 the average separation between a tip apex and a sample surface. According to Eq. (1) the contributions to Δf_{total} from various forces such as F_V, F_{vdw}, F_{bond}, and F_{repul} are additive as $\Delta f_{\text{total}} = \Delta f_V + \Delta f_{\text{vdw}} + \Delta f_{\text{bond}} + \Delta f_{\text{repul}}$. The subscripts indicate the contribution from the respective forces.

Figure 2(a) shows measured Δf plots versus the tip-sample closest separation and the sample bias voltage V. At distant separations larger than 1 nm, the force consists of the van der Waals and the electrostatic forces. For an oscillating tip with respect to a sample, the long-range electrostatic force can be expressed as

$$F_V = \frac{1}{2}\frac{dC}{dz}(V - V_c)^2. \quad (2)$$

Here C is the capacitance between the tip and the sample, z the separation, and V_c the contact potential difference between the tip and the sample. Thus, Δf_V turns out proportional to $(V - V_c)^2$ from Eq. (1), showing a parabolic curve with V. Under a constant oscillation amplitude the proportionality constant dC/dz increases with decreasing separation owing to a steep increase in capacitance. This tendency is confirmed in Fig. 2(a) at the distant separations, and similar parabolic curves have already been reported [20]. Since the van der Waals force does not depend essentially on the bias voltage, the minimum value of Δf at $V = V_c$ ($= -0.27$ V) at a constant distant separation corresponds to the van der Waals force.

On the other hand, the curves of Δf versus bias voltage (nc-AFS spectra) at separations less than about 0.5 nm deviate from their parabolic curves toward stronger attractive force around $V = V_c$ (≈ -0.3 V). Figures. 2(b) and 2(c) show the raw spectra at several separations over a Si adatom and over an area with no Si surface atoms, respectively. In particular, more prominent peaks are found over a Si adatom at specific voltages with decreasing separation, and small sawlike multiple peaks with slightly greater than the noise level are repeatedly found from -0.2 to $+0.8$ V at 0.30 and 0.33 nm. These peaks are possibly attributed to F_{bond}, which exhibits bias dependence and increases with decreasing separation. In addition it is noted that the decay length of force differs with bias voltage at these close separations. Recently, atomic images taken by Kelvin probe microscopy (KPM) have been reported, which depicts the change in a voltage at the bottom of parabolic curve as V_c by evaluating a curve minimum [21,22]. When the curve deviates from a parabolic one, the image instability with hopping between the double minima seems easily induced. This implies that the atomic contrast in KPM images is not directly related to V_c.

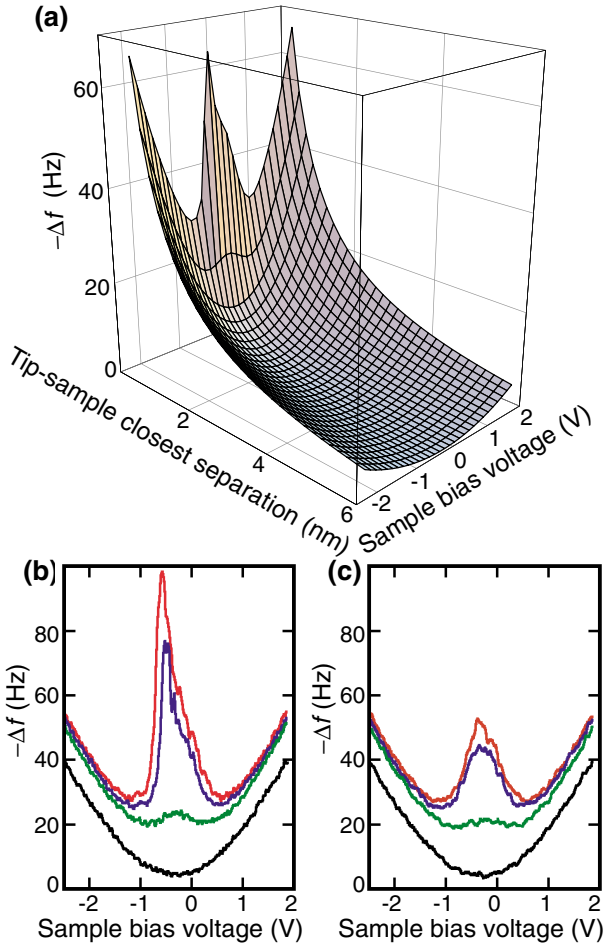

FIG. 2 (color). (a) Δf plots with respect to the tip-sample closest separation and the sample bias voltage, which were measured over a Si adatom on a Si(111)-(7 × 7) surface. Since the force interaction is attractive, Δf negatively increases with decreasing separation. The separation means the closest separation between the sample surface and the apex of tip on an oscillating cantilever. The origin of the separation is estimated from curves of tunneling current versus separation that are experimentally taken by using the same tip and the same sample. (b) Δf curves with respect to sample bias voltage as raw data of nc-AFS over a Si adatom on the Si(111)-(7 × 7) surface with separations of 0.30 (red), 0.33 (blue), 0.43 (green), and 1.5 nm (black), respectively. (c) same as (b) but over an area in which there are no Si surface atoms.

In order to clarify the spectroscopic features for short-range force, we subtract an extrapolated parabolic curve due to the long-range electrostatic force and an offset due to the van der Waals force from the raw curves over several specified positions of surface at a separation of 0.33 nm (Fig. 3). The subtracted curves (short-range force spectra), corresponding to Δf_{bond}, show site dependence with two typical features. One is an attractive broad peak around −0.27 V, which is found everywhere there are no surface atoms [Fig. 3(a)]. The other is a complicated asymmetric peak, which is found over Si adatoms and rest atoms on the Si(111)-(7 × 7) surface [Figs. 3(b) and 3(c)].

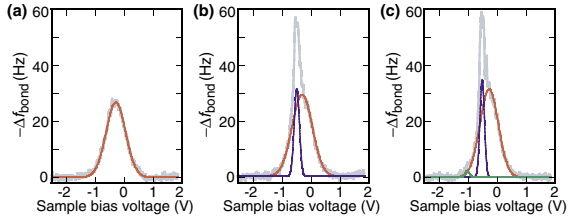

FIG. 3 (color). Short-range force spectra (gray curves) taken at separation of 0.33 nm as in Fig. 2. (a) over an area with no surface atoms, (b) over an adatom, and (c) over a rest atom in a faulted half unit cell on a Si(111)-(7 × 7) surface, respectively, plotted by subtracting a parabolic curve due to electrostatic force and an offset due to the van der Waals force from raw nc-AFS spectra, leading to Δf_{bond}. The curve in (a) is fitted to a numerically calculated Gaussian curve (red). The gray curves are decomposed into a red and a blue curve in (b) and additionally a green curve in (c), which are Gaussian curves as numerically fitted to the gray curves.

By assuming that the spectra consist of several Gaussian peaks, we can decompose the spectra chiefly into a broad peak around −0.27 V with a full width at half maximum (FWHM) of 0.35 V and sharp peaks with a FWHM less than 0.1 V. This indicates that the broad peak is present commonly over the sample surface at separations less than 0.5 nm. On the other hand, the peak voltage of sharp peaks changes on the site as explained in the next paragraph.

According to Chen [5], the quantum mechanical resonance between the surface electronic states of both the tip and the sample through the tunneling barrier is responsible for the force and the tunneling conductance, which is correlated to overlapping of their wave functions at close energy levels. Figure 4(a) shows an energy diagram: the sample surface, Si(111)-(7 × 7), exhibits metallic electronic states, and the [001]-oriented Si tip is semiconducting with an energy gap at its surface. The tip and sample are connected through an external circuit with a voltage power supply; we can control the Fermi level of one body with respect to that of the other body. Thus the resonance between surface electronic states at different energy levels is induced by level tuning with changing bias voltage. The Si adatoms have surface states around the Fermi level, corresponding to the prominent sharp peak at about −0.4 V in Fig. 3(b), and, on one hand, the rest atom with the electronic states around −0.8 eV exhibits a small peak at about −1.0 V in Fig. 3(c) [23,24]. Since the rest atom in the second layer is surrounded by three Si adatoms in the first layer, it is probable that both peaks are found in Fig. 3(c). It is noted that the small sawlike multiple peaks from −0.2 to +0.8 V may correspond to chemical bonding between the spread empty states of the sample and the buckled-up *s*-like orbital (filled states) of the tip.

The origin of the broad peak is possibly attributed to the overlapping of electronic states between the tip and the sample through a lowered tunneling barrier, similar

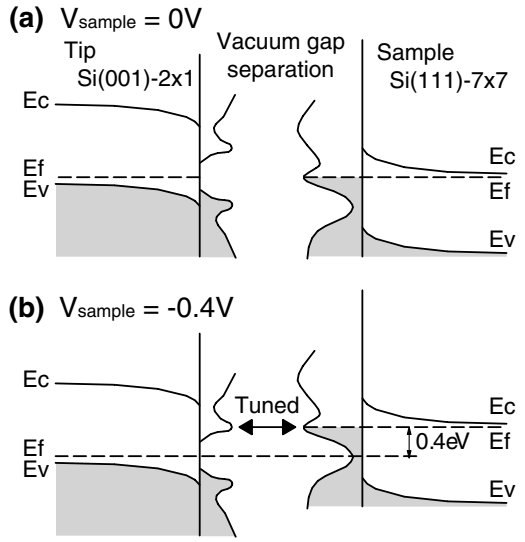

FIG. 4. Simplified tuning energy diagram of a tip of p-Si(001)-(2×1) with an surface energy gap and a sample of n-Si(111)-(7×7) with metallic surface states. (a) $V_{\text{sample}} = 0$ V, and (b) -0.4 V. We assume that the tip states are similar to those on a Si(001)-(2×1) surface with asymmetric dimers. The band gap of Si is about 1.1 eV. The surface Fermi level of the Si(001)-(2×1) and Si(111)-(7×7) is about 0.4 and 0.7 eV above the top of valence band, respectively [25]. Thus the contact potential difference is calculated to be about -0.3 V, which is in good agreement to the measured value of about -0.27 V.

to cohesive resonance energy between metals. From STM experiments, the tunneling barrier decreases typically at separations smaller than 0.5 nm owing to image charge. The resonance through a lowered tunneling barrier enhances the interaction: the resonance indicates that electrons oscillate back and forth between the states of the tip atom and the sample surface atom, where the tunneling electrons are partially backscattered at the potential changes of atoms at the tip apex and the sample surface. These resonating states contribute to the attractive force interaction. Since under a bias voltage compensating the contact potential difference the tunneling barrier is symmetric with a maximum at the center of separation, the resonating interaction is possibly strong. When the bias voltage is increased, that is, the energy regime is in near field emission, the tunneling electrons penetrate deep into bulk beyond the lowered barrier, with less backscattering, resulting in lower attractive force. Detailed theoretical calculations are required to clarify this mechanism.

In conclusion, we found the noticeable bias dependence of the short-range attractive force between two bodies of a tip and a sample at close separations by force spectroscopy with changing bias voltage (nc-AFS). The nc-AFS spectra exhibited prominent features as sharp peaks and a broad peak. The sharp peaks are attributed to quantum mechanical resonance as the energy levels of sample surface states are tuned to those of tip states by shifting the Fermi level through changing bias voltage. The broad peak possibly arises from resonating states over a lowered tunneling barrier. Although the sample in the present study was a semiconductor, the nc-AFS promisingly provides new analytical prospects for force interaction between solid bodies, including metals. In nanotechnology toward characterizing and fabricating new nanostructures such as nanodots and nanocontacts, the bias dependent features of short-range force at small separation hold crucial keys to them, which can be clarified by the nc-AFS. In particular, the energy level tuning by shifting the Fermi level has great potential for atom recognition and manipulation.

This work was supported by Grand-in-Aids for Scientific Research from Japan Society for the Promotion of Science.

[1] L. Pauling, *The Nature of the Chemical Bond* (Cornell University Press, New York, 1960).
[2] G. Binnig *et al.*, Phys. Rev. Lett. **50**, 120 (1983).
[3] G. Binnig, C. F. Quate and C. Gerber, Phys. Rev. Lett. **56**, 930 (1986).
[4] B. Cappella and G. Dietler, Surf. Sci. Rep. **34**, 1 (1999).
[5] C. J. Chen, *Introduction to Scanning Tunneling Microscopy* (Oxford University Press, Oxford, 1993).
[6] U. Dürig, O. Züger, and D. W. Pohl, J. Microsc. **152**, 259 (1988).
[7] C. Loppacher *et al.*, Phys. Rev. B **62**, 16944 (2000).
[8] A. Schirmeisen *et al.*, New J. Phys. **2**, 29.1 (2000).
[9] F. J. Giessibl, Science **267**, 68 (1995).
[10] *Noncontact Atomic Force Microscopy*, edited by S. Morita, R. Wiesendanger, and E. Meyer (Springer, Berlin, 2002).
[11] M. A. Lantz *et al.*, Science **291**, 2580 (2001).
[12] T. Arai and M. Tomitori, Jpn. J. Appl. Phys. Part 1 **39**, 3753 (2000).
[13] T. Arai and M. Tomitori, Jpn. J. Appl. Phys. Part 1 **36**, 3855 (1997).
[14] R. J. Hamers, R. M. Tromp and J. E. Demuth, Surf. Sci. **181**, 346 (1987).
[15] M. Guggisberg *et al.*, Surf. Sci. **461**, 255 (2000).
[16] M. Guggisberg *et al.*, Appl. Phys. A **72**, S19 (2001).
[17] K. D. Brommer *et al.*, Phys. Rev. Lett. **68**, 1355 (1992).
[18] T. Arai and M. Tomitori, Appl. Surf. Sci. **157**, 207 (2000).
[19] F. J. Giessibl, Phys. Rev. B **56**, 16010 (1997).
[20] M. Guggisberg *et al.*, Phys. Rev. B **61**, 11151 (2000).
[21] T. Shiota and K. Nakayama, Jpn. J. Appl. Phys. Part 2 **41**, L1178 (2002).
[22] K. Okamoto *et al.*, Appl. Surf. Sci. **210**, 128 (2003).
[23] Ph. Avouris, I. W. Lyo and F. Bozso, J. Vac. Sci. Technol. B **9**, 424 (1991).
[24] M. Fujita, H. Nagayoshi and A. Yoshimori, Surf. Sci. **242**, 229 (1991).
[25] H. Lüth, *Surfaces and Interfaces of Solid Materials* (Springer, Berlin, 1995).